Ocean Engineering 86 (2014) 58–67

Contents lists available at ScienceDirect

Ocean Engineering

journal homepage: www.elsevier.com/locate/oceaneng

Uncertainties related to predictions of loads and responses for ocean and offshore structures

Wei Qiu [a,*], Joel Sales Junior [b], Dongyeon Lee [c], Halvor Lie [d], Viacheslav Magarovskii [e], Takashi Mikami [f], Jean-Marc Rousset [g], Sergio Sphaier [b], Longbin Tao [h], Xuefeng Wang [i]

[a] Memorial University, Canada
[b] Universidade Federal do Rio de Janeiro, Brazil
[c] Samsung Ship Model Basin, Republic of Korea
[d] Marintek, Norway
[e] Krylov State Research Center, Russia
[f] Akishima Laboratories (Mitsui Zosen) Inc., Japan
[g] Ecole Centrale de Nantes, France
[h] Newcastle University, UK
[i] Shanghai Jiao Tong University, China

ARTICLE INFO

Article history:
Received 13 March 2013
Accepted 22 February 2014
Available online 12 April 2014

Keywords:
Ocean engineering model tests
Full-scale tests
Numerical simulations
Uncertainty analysis methods

ABSTRACT

This paper discusses uncertainties related to the prediction of loads and responses for ocean and offshore structures in accordance with the findings by the Ocean Engineering Committee of the International Towing Tank Conference (ITTC). The parameters that may cause uncertainties in ocean engineering model tests, full-scale tests and numerical simulations are presented in terms of physical properties of the fluid, initial conditions, model definition, environment, scaling, instrumentation and human factors. Emphasis is given to the uncertainty sources in model tests involving deepwater mooring lines, risers and dynamic positioning systems and the need for quantifying them. A methodology for uncertainty analysis is described according to the International Organization for Standardization (ISO) Guidance for Uncertainties in Measurement (GUM). As an example of application, the combined and expanded uncertainties in the model tests of a moored semi-submersible platform were assessed and quantified in terms of motion responses, air gap and mooring line tensions. It is concluded that the quantification of uncertainties may be challenging in model tests and numerical simulations of ocean and offshore structures. It is particularly challenging in extrapolating model test results to full scale and utilizing complex numerical models, especially if the effects of hydrodynamic nonlinearities are significant.

1. Introduction

The prediction of loads and responses is of importance in the design and operation of ships and offshore structures in the ocean environments. Uncertainties in the prediction are one of the main concerns of the shipping and offshore industry.

The responses of structures in ocean environments can be predicted using model tests, numerical simulations and full-scale tests. There are many parameters that cause uncertainties in the experiments and numerical simulations. It is important to identify these parameters and quantify the uncertainties.

The International Ship and Offshore Structures Congress (ISSC) and the International Towing Tank Conference (ITTC) jointly held a workshop in 2012 with an aim to understand the uncertainties in the description of environment, predictions of loads and responses of marine structures, and risk assessment and mitigation in design and operation. As one outcome of the Workshop, this paper presents the uncertainties related to predictions of loads and responses for ocean and offshore structures identified by the ITTC Ocean Engineering Committee. The focus is on uncertainties related to tests and simulations of bottom-founded structures, stationary floating structures with mooring lines or dynamic positioning systems, and renewable energy systems.

There have been many model tests, full-scale experiments and numerical simulations on ocean and offshore structures in recent years. For example, Morgan and Zang (2010) investigated the use of a computational fluid dynamics (CFD) software suite for the simulation of focused wave packets interacting with a vertical bottom mounted cylinder. Yang et al. (2010) reported on the experimental study of the scour around jacket offshore wind turbine foundations in shallow water and in different wave and current conditions. The effect of scour mitigation devices was

* Corresponding author.
E-mail address: qiuw@mun.ca (W. Qiu).

http://dx.doi.org/10.1016/j.oceaneng.2014.02.031
0029-8018

Nomenclature

EA	mooring line axial stiffness
EI	mooring line bending stiffness
DOF	degree of freedom
f	an experimental result
ISO	International Organization for Standardization
ISSC	International Ship and Offshore Structures Congress
ITTC	International Towing Tank Conference
RAO	response amplitude operator
T_2	measured tension of mooring line #2
T_8	measured tension of mooring line #8
T_2'	tension RAO of mooring line #2
T_8'	tension RAO of mooring line #8
t_{95}	coverage factor at 95% confidence level.
$\mathbf{x}_n$	measured variables
x_3	measured heave
x_3'	heave RAO
x_{ag}	measured air gap
x_{ag}'	air gap RAO
u_c	combined uncertainty
u_e	expanded uncertainty
u_f	uncertainty of experimental result, f
η_a	wave amplitude
ν_{eff}	effective number of DOF
ν_i	estimated number of DOF

investigated. Roos et al. (2009, 2010) reported on the experimental study of wave impacts on elements of a gravity-based structure (GBS), composed of submerged storage caissons combined with four surface piercing vertical cylinders, in relatively shallow water. The wave impact loads on deck and the loads on vertical columns were successively investigated. Hussain et al. (2009) presented the measured steady drift force and low frequency surge motions of a semi-submersible model. A complete review of recent tests and numerical simulations of bottom-founded structures, stationary floating structures and renewable energy systems can be found in the final report of Ocean Engineering Committee, 26th ITTC (2011).

In this paper, parameters that may cause uncertainties in ocean engineering model tests, full-scale tests and numerical simulations are identified in terms of physical properties of fluid, initial conditions, model definition, environment, scaling, instrumentation and human factors. Parameters with dominant contributions to uncertainties in model tests involving deepwater mooring lines and risers and dynamic positioning systems are discussed. A uncertainty analysis methodology is described according to the ISO guidance. As an example, the uncertainty analysis method was applied to the tests of a moored semi-submersible platform model. The combined and expanded uncertainties were quantified in experimental results including motion responses, air gap and mooring line tensions. Challenges have also been identified in quantifying the uncertainty sources in tests and numerical simulations of ocean and offshore structures.

2. Parameters causing uncertainties in ocean engineering tests

Various methodologies can be applied to predict the response behavior and loads acting on ocean and offshore structures, including model experiments, full-scale measurements and theoretical methods. A comprehensive review of these methods can be found in Hirdaris et al. (2014). There are many parameters that can cause uncertainties in tests and numerical simulations based on these methods. The parameters causing uncertainties in ocean engineering model tests, full-scale tests and numerical simulations are discussed below and presented in Table 1 according to the categories of physical properties of fluid, initial conditions, model definition, environment, scaling, instrumentation and human factors.

2.1. Model tests

A review of issues associated with accuracy of physical modeling based on model tests can be found in the work of Vassalos (1999). In terms of categories listed in Table 1, sources of uncertainties in model tests are described below.

In the category of physical properties of water, these parameters include viscosity, density, temperature, surface tension, aeration, seeding or contamination.

The initial test conditions, such as remaining waves, circulation and turbulence in the tank from previous tests, can cause uncertainties.

There are many parameters in the model definition. For models with mooring lines and risers, the uncertainties can be caused by bottom friction of mooring lines, truncation of mooring lines, length, diameter, weight distribution, stiffness distribution, structural scaling, friction in bearings, location of anchor point, fairlead position, and pretension. The hull geometry and its GM value with and without mooring lines/risers, the inertia and stiffness properties, the topside geometry, the surface roughness, the thruster geometry and control systems, as well as the speed and the heading of the model are also the key parameters.

In terms of environment effects, the key parameters include wave conditions which are usually only measured at defined points, parasitic waves on shallow water, variation of current in time and space, wind conditions in terms of homogeneity and profile, wave-maker control, wave reflection from beaches and model, interaction between wind and waves, refraction due to uneven seabed on shallow water, wave–current interaction, and

Table 1
Uncertainty sources.

Method	Category	Example of source
Model tests	Physical properties of fluid	Viscosity
	Initial test conditions	Remaining waves
	Model definition	Hull geometry
	Environment	Wave modeling
	Instrumentation	Sensors
	Scaling	Viscous effect
	Human factors	Manual heading control
Full scale tests	Physical properties of fluid	Density
	Environment	Wave measurement
	Instrumentation	Position and synchronization
	Human factors	Crew behavior
Numerical modeling	Chosen governing equations	Limitation on describing the physics
	Numerical methods	Level of approximation
	Numerical implementation	Grid generation and distribution
	Calibration of parameters	Empirical parameter input
	Computing infrastructure	Computing capacity
	Human factors	Understanding of numerical model

test duration which affects the quality of generated environment. The statistical uncertainties also contribute to the environmental realization. It is known that extreme values in particular may have large uncertainties.

Instrumentation, such as gauges, transducers and optical systems, can cause uncertainties in measurements in terms of accuracy and calibration of gauges, stability of instrument, parasitic vibrations and noises, positions of transducers and the accuracy of the optical systems.

Another possible source of uncertainty is scaling, where the physical similarity cannot be kept, such as viscous effect.

Human factors may also play important roles in the uncertainties of measurements, for example, manual heading control in self-propelled seakeeping or maneuvering tests. Moreover, the analysis of the results and the decisions made based on experience and judgment may cause bias input to the results of model tests. One example of human factor is that some good data may be wrongly taken as outlier due to poor judgment. However, this issue is rarely addressed in the literature of ocean engineering experiments. Some insights may be taken from other areas such as decision-making and cognitive bias problems in behavioral economics. The concept of uncertainty due to judgement was given in the work of Tversky and Kahneman (1974). A recent application of their concept is presented in the work of Elms and Brown (2013).

2.2. Full-scale tests

The uncertainty sources in the full-scale tests are similar to those in the model tests including the physical properties of fluid, environment, instrumentation, and human factors. For environment, the levels of uncertainties could be more significant in measurements of waves, currents and wind in full scale. Other sources of uncertainties are due to the constrains in positions of instrumentation and the synchronization of measurements. For human factors, the crew behavior also contributes to uncertainties in measurements.

2.3. Numerical modeling

The uncertainty sources in numerical modeling are in different nature from those in the model and full-scale tests. A review of numerical methods can be found in Hirdaris et al. (2014). The errors in modeling can be caused by the chosen equations to describe real physics, the choice of numerical/theoretical method, the level of approximation, the type of turbulence models, the grid generation and distribution, the rounding error, the amount of effort and computing capacity, the introduction of empirical parameters, and the understanding of the physical model and the numerical model by the user.

3. Parameters causing large uncertainties in model tests

In this section, we focus on identifying the parameters with dominant contributions to uncertainties in model tests involving mooring lines and risers in deepwater and dynamic positioning systems. A summary of uncertainty sources in these tests is given in Table 2.

3.1. Uncertainties in model tests involving mooring lines and risers

When testing structures with mooring lines, risers or other submerged lines, especially for deepwater, the primary requisite is to correctly model the system's line force characteristics, i.e., forces and moments due to linear and angular offsets of the moored structure. Many uncertainties are involved in this stage, especially

Table 2
Uncertainty sources in model tests involving deepwater mooring lines/risers and dynamic positioning (DP) systems.

Test Type	Source	Comments
Mooring system	Line static characteristics	Due to truncation of the lines
	Line dynamic characteristics	Due to truncation and scale effect
	Position of anchor points	Due to errors in positions at basin
	Load cell influence	Due to sensor weight and induced flow
	Truncation of lines	Due to differences between truncated and full-depth systems
DP system	Scale effects on propellers	Due to scaling based on Froude's similitude
	Hydrodynamic effects on propellers	Their interactions with model and prototype are different, such as suction
	Control parameters	Control algorithms/parameters are different for model and prototype
	Model limitation	Due to lack of space for the DP system
	Control feedback values	Model and prototype use different values

when the truncation of lines is needed in deepwater cases, since it is difficult to scale the elastic and mass characteristics of prototype lines. To scale the elasticity, the axial and flexural stiffness, EA and EI, when they are important, and the mass (density) in the same time, it is often required to change the specified segment configuration of each line, or even to bundle some very thin lines in groups. This leads to the addition of spring segments, the partial or total substitution of original segments, and sometimes the addition of floaters or clump weights in some segments to correct submerged weight.

The instrumentation of mooring lines also causes some uncertainties, for example, in-line load cells are often used to measure line tensions. The geometry and the weight of such sensors change the properties of the line segment where the sensors are located.

Another source of uncertainty is the location of an anchor point on the basin bottom. Special care has to be paid to the correct marking of anchor points and water depth of mooring lines. The bottom friction coefficient also contributes to this.

For model tests with truncated mooring lines/risers, it is important to keep the correct geometrical parameters of the system, i.e., top angles and lines elongation during excursion. This may lead to other distortions on the originally specified characteristics of segments. In some cases, a totally different mooring system from the prototype one may be used.

In addition to the uncertainty sources associated with the restoring force issues in the design of scaled submerged lines, there are other sources related to the hydrodynamic loads on the lines, for example, the current loads and the damping contribution to the total damping of the system. The drag of the segments may play an important role in the behavior of the floater, especially when the number of mooring lines and riser is large and/or the floater damping is small compared to the line damping. In this case, the truncation will lead to more uncertainties due to geometric differences on segments and great changes of the configuration of the mooring lines. To assess the drag of the modeled lines, an analysis of the Reynolds number on each segment will be necessary and some distortion on diameters may be needed to correct the drag effects.

An improved method for the prediction of responses from model tests with a truncated deepwater floating system is to apply the hybrid verification technique (Ormberg et al., 1999; Stansberg

et al., 2002) that combines model tests with numerical simulations. The hybrid method involves (1) the design of truncated mooring and riser system and performing model tests with the truncated system; (2) numerical reconstruction of truncated model tests and the estimation of hydrodynamic properties from the tests and the correlation and calibration of a numerical model against the test results. This includes the static and dynamic reconstructions of responses of individual lines as well as the static and dynamic behavior of the total system. A simulation program designed for the fully non-linear coupled analysis is recommended to be used for this purpose; and (3) numerical extrapolation to the full depth system using the calibrated numerical model.

It should be noted that the acceptance of uncertainty in the testings involving mooring lines and risers depends on the objective of the tests. For example, for the first-order motions, these levels of uncertainties may be acceptable. However, the uncertainties may be considered large for drifting forces.

3.2. *Uncertainties in model tests involving dynamic positioning systems*

There are many factors causing uncertainties in model tests involving dynamic positioning (DP) systems.

The first issue is on the floater itself which is usually tested in low velocities. This may lead to great scale effects due to friction forces acting on the hull.

The second issue is the modeling of thrusters and propellers whose hydrodynamic characteristics are not necessarily well described by the Froude scale law as discussed in Vassalos (1999). Even if the thrust forces are correctly modeled according to the Froude scale, other uncontrolled effects on the flow of each propeller and on the thruster–thruster and thruster–hull interactions may affect the behavior of the overall system.

The third issue is on the modeling of the electronic control system. Usually the parameters used in the DP system of a prototype are tuned in a very empirical way and are based on the experience of the DP system manufacturer. These parameters are often not available for the model tests. Even when they are known, they will have to be adapted to the model system. As the control parameters are directly related to the behavior of the system, special care is needed. There are also uncertainties associated with the feed values of model position which is usually measured by an optical tracking system and other parameters, for example, wind velocity and wave heights. It is desirable that these values are treated to give correct levels of input noise to simulate the same uncertainty observed in prototype, for example, the GPS and other equipment errors. It is also beneficial to assess the influence of the uncertainty on the behavior of the control system by changing the level of noise on the feed values.

Based on the issues discussed above, the main factors affecting the uncertainties in DP tests are listed below:

- Scale effects on model friction forces due to low Reynolds number.
- Hydrodynamic effects of propellers and thrusters which are uncontrolled effects due to thruster–thruster interaction and thruster–hull interaction.
- Propeller air suction effects.
- Propeller emersion effects.
- Control parameters of model and prototype. The control parameters of a prototype from DP manufacturers are often not available for model tests.
- Bundling propellers or changing of propeller/thruster position due to space limitation of model.
- Quality of feed values used in the control system of the model different from those of the prototype.

Similar to the model tests involving mooring lines and risers, the acceptance of uncertainty level also depends on the objective of a test.

4. A methodology for uncertainty analysis

According to the ISO-GUM methodology (ISO, 2008), the expression of uncertainties in measurements is based on five principles:

(1) The uncertainty results may be grouped into two categories, Type A uncertainty and Type B uncertainty. The Type A uncertainties are those evaluated by applying statistical methods to the results of repeated measurements. The Type B uncertainties are those evaluated by means other than the statistical methods. The associated estimated variance or the standard uncertainty is evaluated by scientific judgement according to the available information, which may include the previous measurement data, experience or knowledge of instruments or materials, information provided by the manufacturers, data obtained in calibration or from other certificates, and uncertainties assigned to reference data from handbooks or manuals.
(2) The components in Type A uncertainties are defined by the estimated variance including the effect of the number of degrees of freedom.
(3) The components in Type B uncertainties are also approximated by a corresponding variance, in which its existence is assumed.
(4) The combined uncertainty should be computed by the normal method for the combination of variances, known as the law of propagation of uncertainty.
(5) For particular applications, the combined uncertainty should be multiplied by a coverage factor to obtain an overall uncertainty value. Note that the overall uncertainty is called expanded uncertainty.

Based on these principles, the uncertainty analysis can be carried out to obtain the uncertainty in a measurement. Assuming an experimental result, f, is a function of n measured variables, $\mathbf{x}_n$, i.e., $f=f(x_1, x_2, \ldots, x_n)$. The uncertainty, u_f, in the results can be calculated by

$$u_f^2 = \left(\frac{\partial f}{\partial x_1}\right)^2 u_{x_1}^2 + \left(\frac{\partial f}{\partial x_2}\right)^2 u_{x_2}^2 + \ldots + \left(\frac{\partial f}{\partial x_n}\right)^2 u_{x_n}^2 \quad (1)$$

where u_{x_n} is the uncertainty in x_n. Therefore, if the result is given by a reduction function f, the final uncertainty can be calculated by Eq. (1), which covers all uncertainties if all of their sources are related to the measured variables, $\mathbf{x}_n$. However, for most problems, one can identify various sources that are not directly related to measured variables, but in some way influence their uncertainties u_{x_n}. This can be expressed mathematically as follows:

$$x_n = g_n(y_1, y_2, \ldots, y_n) \quad (2)$$

and

$$u_{x_n}^2 = \left(\frac{\partial g_n}{\partial y_1}\right)^2 u_{y_1}^2 + \left(\frac{\partial g_n}{\partial y_2}\right)^2 u_{y_2}^2 + \ldots + \left(\frac{\partial g_n}{\partial y_n}\right)^2 u_{y_n}^2 \quad (3)$$

where x_n are the measured variables presented in the reduction equation (1) and y_n are variables related to other sources of uncertainties that affect x_n and are described by functions g_n.

The main issue on deriving or estimating $\partial g_n/\partial y_n$ and u_{y_n} is that they would need extensive effort and resources, because the analytical functions, g_n, are not necessarily available, i.e., cannot be explicitly expressed in terms of y_n.

Note that a pure Type A analysis could also be performed so that no derivatives are needed. However, this type of analysis

should be carried out in such a way that all of the uncertainty sources are taken into account in the standard deviation of the samples. This will require to treat all of those sources in the test matrix as random variables, i.e., the sampling process should account for the variations in all the uncertainty sources. For instance, to include the effect of uncertainty on the hull geometry in the Type A analysis, one may use different models in the tests so that the uncertainty on geometry can be included in the final standard deviation of the results. As another example, any possible bias from the test set-up should be included in the analysis by assembling and dismantling each set-up and by using different set-ups.

As the resources for performing tests are limited, it is often not feasible to conduct the pure Type A tests. The final uncertainties will usually combine Type A and Type B sources.

To illustrate this issue, a simple uncertainty analysis was carried out for a semi-submersible model test, where the reduction function is the response amplitude operator (RAO) given below:

$$\mathrm{RAO} = f(x, \eta_a) = \frac{x}{\eta_a} \tag{4}$$

where x is the mean amplitude of a variable, such as heave motion amplitude and η_a is the mean wave amplitude.

If one analyzes the tests in which x and η_a are measured, a few sources listed in Tables 1 and 2 that affect x and η_a shall be taken into account. For instance, if x is the heave motion, x_3, and η_a is the measured wave amplitude during a regular wave test, some of those sources affecting the uncertainties of x_3 and η_a, $u(x_3)$ and $u(\eta_a)$, would include water density, reflected waves, nonlinearity of waves, wave direction, model geometry, mooring forces and so on, besides the uncertainties in their direct measurements.

Based on Eq. (2), the heave motion x_3 and the wave amplitude, η_a, can be written as below in terms of these sources of uncertainty

$$x_3 = g_1(y_1, y_2, y_3, y_4, y_5) \tag{5}$$

where y_n, $n = 1, 5$, represent the sources due to motion measurement, water density, model geometry, mooring forces and wave direction, respectively; and

$$\eta_a = g_2(y_2, y_6, y_7, y_8) \tag{6}$$

where y_6, y_7 and y_8 are the uncertainty sources due to wave measurement, wave reflection and wave nonlinearities, respectively.

Therefore, the uncertainties, $u(x_3)$ and $u(\eta_a)$, can be written as

$$u_{x_3}^2 = \left(\frac{\partial g_1}{\partial y_1}\right)^2 u_{y_1}^2 + \left(\frac{\partial g_1}{\partial y_2}\right)^2 u_{y_2}^2 + \cdots + \left(\frac{\partial g_1}{\partial y_5}\right)^2 u_{y_5}^2 \tag{7}$$

$$u_{\eta_a}^2 = \left(\frac{\partial g_2}{\partial y_2}\right)^2 u_{y_2}^2 + \left(\frac{\partial g_2}{\partial y_6}\right)^2 u_{y_6}^2 + \left(\frac{\partial g_2}{\partial y_7}\right)^2 u_{y_7}^2 + \left(\frac{\partial g_2}{\partial y_8}\right)^2 u_{y_8}^2 \tag{8}$$

The partial derivatives, $\partial g_1/\partial y_n$ and $\partial g_2/\partial y_n$, represent the sensitivity of $u(x_3)$ and $u(\eta_a)$ to variables, y_n, respectively.

Since the analysis was not extended to the sources not presented in the reduction equation, the Type B uncertainty was only calculated accounting for the uncertainties in the direct measurements of x and η_a, i.e., only the terms due to uncertainties in direct measurements, $(\partial g_1/\partial y_1)^2 u_{y_1}^2$ for x_3 and $(\partial g_2/\partial y_6)^2 u_{y_6}^2$ for η_a, were considered. The same simplifications were applied to all other calculations.

The procedure for a typical Type B uncertainty analysis is given as follows:

1. Identification of uncertainty sources (for registry).
2. Identification of reduction equation.
3. Estimation of standard uncertainties for each variable in the reduction equation.
4. Estimation of degrees of freedom for each variable identified in Step 3.
5. Calculation of partial derivatives from the reduction equation.
6. Calculation of the final uncertainties using Eq. (1).
7. Calculation of the final degree of freedom for uncertainty analysis.
8. Calculation of the coverage factor using the value calculated in Step 7.
9. Calculation of the final expanded Type B uncertainty.

The degrees of freedom mentioned in Steps 4 and 7 are defined in ISO (2008) and are used to estimate the standard uncertainties from different sources.

For the Type A analysis, an end-to-end approach is applied, i.e., the standard deviation of final values calculated from the reduction equation is used to estimate the scattering of results.

5. Uncertainty analysis on model tests of a moored semi-submersible

As an example, this paper presents the uncertainty analysis on model tests of a moored semi-submersible platform carried out at the LabOceano, Brazil (Kendon et al., 2008). Both Type A and Type B uncertainties in RAO calculations were identified and quantified. Uncertainties in some of the results such as heave RAO, mooring line tensions and air gap measurements are presented. The semi-submersible model shown in Fig. 1 is in 1:100 scale. It was tested with three different mooring systems, i.e., horizontal mooring, truncated mooring and full depth mooring, as shown in Fig. 2. The mooring line numbering is also presented in Fig. 1. The model was tested in both regular waves and irregular waves.

The wave basin and the model were instrumented for the measurement of 6 degree-of-freedom (DOF) motions, air gaps at specific locations and the mooring line tensions at the top of the lines close to the fairlead positions. The virtual tracking system and the infra-red target at the model were used to measure the platform motions.

5.1. Uncertainty sources

The main factors affecting the uncertainties in the tests of the semi-submersible model are listed below.

Model geometry: The maximum allowed dimensional deviation was chosen as 1.5 mm based on the experiences in the model fabrication and tests. It is believed that this deviation will lead to minor effects on model behavior since it has little influence on submerged volume, the center of buoyancy, model symmetry and model displacement.

Model calibration: The maximum allowed mass deviation was considered as 0.5% of the displacement, while the deviations for the center of gravity (CG) and the moment of inertias were 2 mm and 3.5%, respectively. Note that all the masses and moments of inertia of the instruments and accessories were taken into account.

Waves calibration: The calibrated waves were measured using wave gauges with uncertainties of less than 0.5 mm. The maximum deviation of wave height has been identified as 5% and the maximum deviation of wave period was estimated at 1%. The wave absorption by the beaches was estimated at 95%.

Motion measurements: A visual tracking system was used to measure 6 DOF motions of the model. The system uncertainties were estimated as less than 0.5 mm for linear motions and 0.05° for angular motions.

Mooring lines effects: By using the horizontal mooring system, it may be expected that the model will keep its position and heading and the motions can be measured corresponding to correct incident wave characteristics. On the other hand, the mooring system may be stiff in roll and pitch so that the semi-submersible model may interfere

with the angular restoring forces (Stansberg et al., 2002). Therefore, the increase in hydrostatic restoring moments by the horizontal mooring system has to be determined. For some cases, heave motions may also be affected. In the current tests, it was assumed that 2% influence on angular stiffness would be acceptable based on experiences. This was checked by performing an inclining test on free floating model and then comparing it with the moored model.

Scale effects: As the model tests were performed according to Froude's law, it is known that the Reynolds dependent phenomena may not be correctly represented. It was assumed that the scale effect is negligible for the semi-submersible model. For the mooring lines, due to the low Reynolds numbers, the mooring damping would be over-estimated, which may decrease the model motions.

Set-up uncertainties: The position and heading of the model was checked before each test. This was done with reference to the lines crossing the basin walls and by using the calibration tools for the visual tracking system. Positions of all wave probes at basin were also checked. It was allowed a maximum deviation of 5 mm in OX and OY directions (in a plane parallel to water surface) and 2 mm in OZ direction. The model draft was verified and a maximum deviation of 1 mm was allowed. For mooring lines, anchor positions were also checked using the same criteria as for the positions of wave probes.

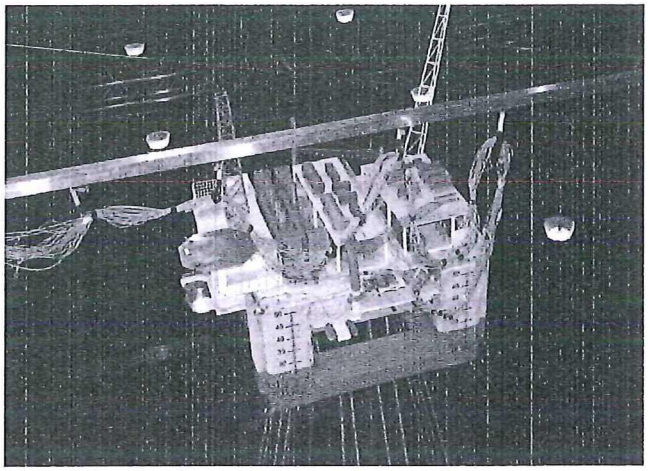

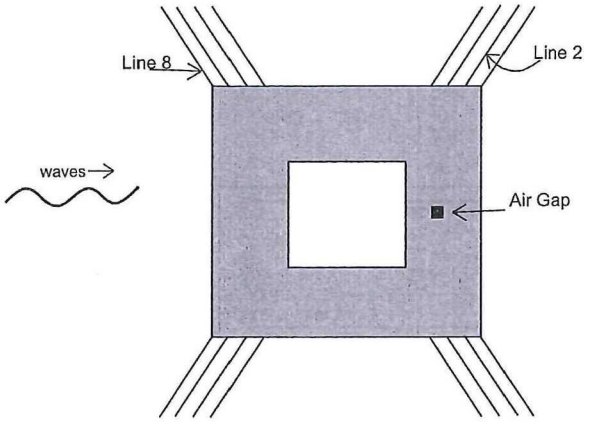

Fig. 1. The semi-submersible model and the mooring line numbering.

5.2. Type A uncertainties

As an example, the Type A uncertainties of measurements such as heave, air gap and mooring line tensions were calculated for the wave period of 10 s(full scale) by considering a series of tests as different realizations.

As only one regular wave was generated during the tests, the irregular-wave test results were also used for the Type A analysis, where the RAO was calculated using the following expression:

$$\mathrm{RAO}_x(T) = \left(\frac{S_x(T)}{S_\eta(T)}\right)^{0.5} \tag{9}$$

where T is the wave period, S_x is the measured power spectral density of the response, x, and S_η is the measured power spectral density of wave elevation, η.

The spectral functions, S_x and S_η, were calculated with the periodogram method(Welch, 1967), using a 3-h time series waves divided into sets of 2048 (TEST 2–5 as shown in Table 3)

Table 3
Full-scale heave, air gap and maximum tension RAO's at $T=10$ s.

	x'_3 (m/m)	x'_{ag} (m/m)	T'_2 (kN/m)	T'_8 (kN/m)
TEST 1	0.2577	1.813	8.79	10.06
TEST 2	0.2286	1.373	6.06	10.21
TEST 3	0.2299	1.542	6.35	9.47
TEST 4	0.241	1.446	*6.41	8.51
TEST 5	0.2224	1.435	6.95	9.01
TEST 6	0.2764	1.277	6.21	9.38
TEST 7	0.2399	1.504	5.64	9.08
TEST 8	0.2822	1.337	5.44	8.52
TEST 9	0.2838	1.31	6.21	10.06
Mean	0.241	1.435	6.21	9.38
σ	0.0243	0.1626	0.98	0.64
u	0.0081	0.05421	0.33	0.21

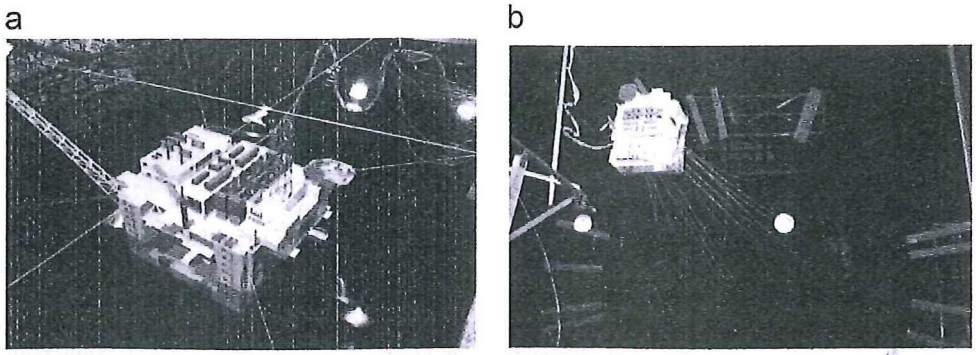

Fig. 2. Mooring line arrangement. (a) Horizontal mooring and (b) full depth mooring.

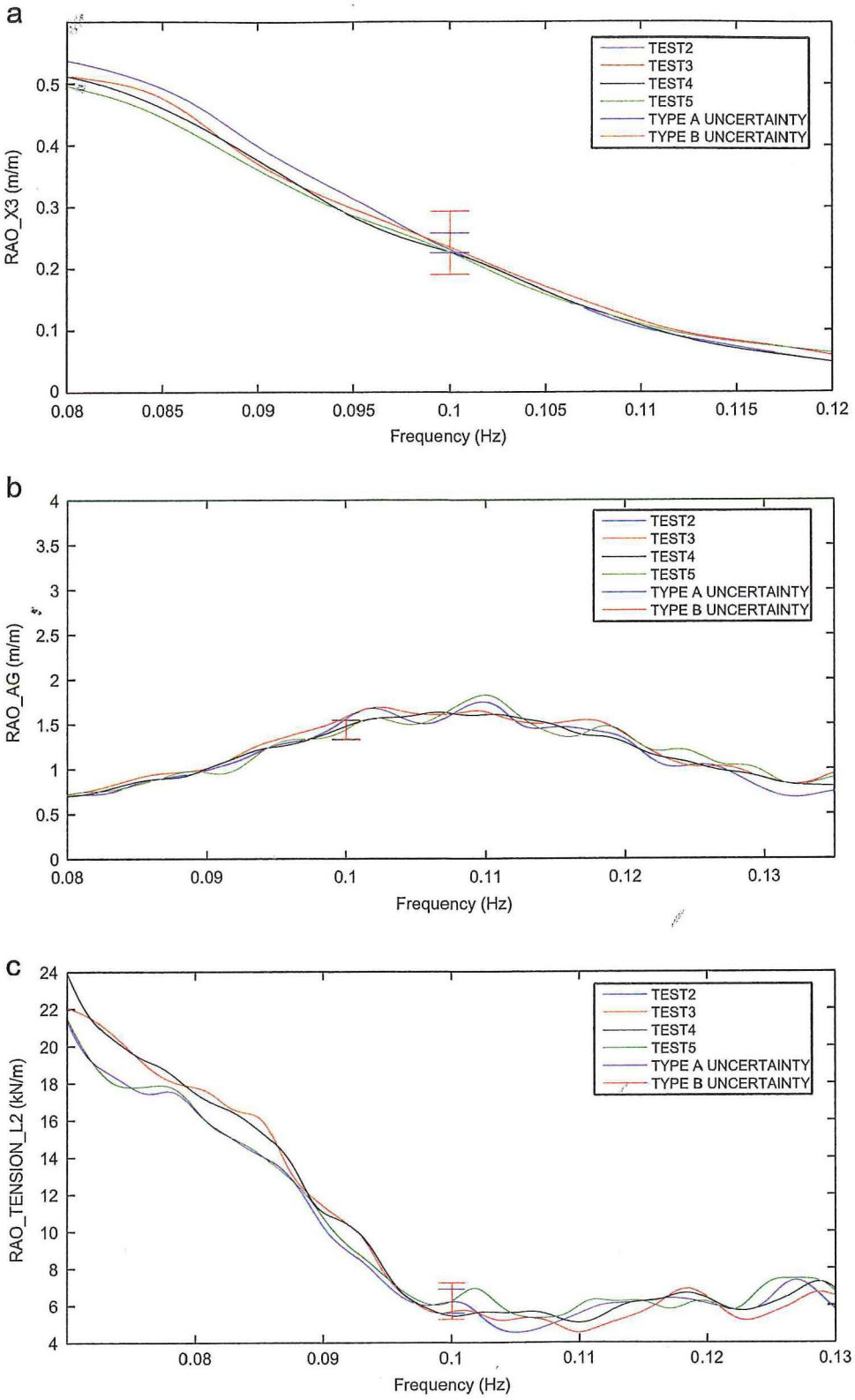

Fig. 3. Uncertainty bars. (a) Heave RAO, (b) air gap RAO and (c) tension RAO of mooring line #2.

or 1024 data points (TEST 6–9) with hanning windows and 10% overlapping. Different parameters were input to the analysis accounting for uncertainties in smoothing spectral curves.

The Type A uncertainties in full scale based on different methods are presented in Table 3. In TEST1, a regular wave was generated, while irregular waves using different wave spectra were tested in TEST 2–TEST 5. The RAO's of heave, air gap and line tensions at lines 2 and 8 were calculated based on the 32 DOF analysis. In TEST 6–TEST 9, RAO's were calculated with the 64 DOF analysis. Note that TEST 5 was the same realization as TEST 1, TEST 6 was the same as TEST 2 and so on.

Table 4
Expanded type A and type B uncertainties in full scale at $T = 10$ sec

	$u_e(x'_3)$	$u_e(x'_{ag})$	$u_e(T'_2)$
Unit	m/m	m/m	kN/m
Type A	0.0161	0.108	0.650
Type B	0.0514	0.103	1.084

In Table 3, σ is the standard deviation, u is the standard uncertainty, x'_3 is the heave RAO, x'_{ag} is the air gap RAO, and T'_2 and T'_8 are the maximum tension RAO's of lines 2 and 8, respectively.

Note that it is assumed that there is a linear relation between the wave elevation and the responses. This consequently contributes to the uncertainty results.

5.3. Type B uncertainties

To take into account calibration uncertainties from the instrumentation, the analysis of Type B uncertainties was performed for the RAO results.

The Type B uncertainties for heave and air gap RAO's were from the calibration of the visual tracking sensors and the wave probes. For mooring line tensions, the uncertainties considered were those from the load cells and the wave probes.

The standard uncertainties assumed for the measured variables in full scale were given by $u(x_3) = 0.05$ m , $u(T_2) = u(T_8) = 1$ KN, and $u(\eta_a) = 0.05$ m based on the basin experience, according to the scale of 100. Their model-scale values are 0.5 mm, 0.001 N and 0.5 mm, respectively.

5.4. Combined type B uncertainties

To calculate the combined uncertainties, the standard uncertainties obtained in Table 3 were used. The reduction equations are as follows:

$$x'_3 = f(x_3, \eta_a) = x_3/\eta_a \tag{10}$$

$$x'_{ag} = f(x_{ag}, \eta_a) = x_{ag}/\eta_a \tag{11}$$

$$T'_2 = f(T_2, \eta_a) = T_2/\eta_a \tag{12}$$

where x_3, x_{ag} and T_2 are the measured heave, air gap and tension at mooring line 2, respectively. The combined standard uncertainties for RAO's, $u_c(x'_3)$, $u_c(x'_{ag})$ and $u_c(T'_2)$ are

$$u_c^2(x'_3) = \left(\frac{\partial x'_3}{\partial x_3}\right)^2 u^2(x_3) + \left(\frac{\partial x'_3}{\partial \eta_a}\right)^2 u^2(\eta_a) = \left(\frac{1}{\eta_a}\right)^2 u^2(x_3) + \left(\frac{x_3}{\eta_a^2}\right)^2 u^2(\eta_a) \tag{13}$$

$$u_c^2(x'_{ag}) = \left(\frac{\partial x'_{ag}}{\partial x_{ag}}\right)^2 u^2(x_{ag}) + \left(\frac{\partial x'_{ag}}{\partial \eta_a}\right)^2 u^2(\eta_a) = \left(\frac{1}{\eta_a}\right)^2 u^2(x_{ag}) + \left(\frac{x_{ag}}{\eta_a^2}\right)^2 u^2(\eta_a) \tag{14}$$

$$u_c^2(T'_2) = \left(\frac{\partial T'_2}{\partial T_2}\right)^2 u^2(T_2) + \left(\frac{\partial T'_2}{\partial \eta_a}\right)^2 u^2(\eta_a) = \left(\frac{1}{\eta_a}\right)^2 u^2(T_2) + \left(\frac{T_2}{\eta_a^2}\right)^2 u^2(\eta_a) \tag{15}$$

For illustration, the results were only calculated for the regular wave test, since there is no reduction equation for irregular waves. In the calculations, it was assumed that there is no correlation between the variables. Considering η_a=2.011 m in full scale and using measured values (full scale) from TEST 1 as given in Table 3, x'_3 = 0.2577 m/m, x'_{ag}= 1.813 m/m and T'_2= 8.79 kN/m, the combined uncertainties in full scale for x'_3, x'_{ag} and T'_2 can be found as 0.0257 m/m, 0.0515 m/m and 0.543 kN/m, respectively.

5.5. Expanded uncertainties

Expanded uncertainties are the final uncertainty values, calculated from the standard uncertainty values and multiplied by the so-called coverage factor (ISO, 2008). The coverage factor relates the standard value to a function of probability distribution so that one can estimate the uncertainty associating its value with a given confidence level, by using a t-distribution with ν degrees of freedom.

Therefore, the expanded uncertainty u_e becomes

$$u_e = k(\nu)u_c \tag{16}$$

where u_c is the combined uncertainty, $k(\nu)$ is the coverage factor, and ν is the number of degrees of freedom for the coverage factor.

For Type A uncertainties, the number of degrees of freedom for the coverage factor is based on the number of data points. For example, as shown in Table 3, the number of degrees of freedom for the t-distribution will be 8 for 9 data points. It gives a coverage factor of 2.3.

For Type B combined uncertainties, the coverage factor also depends on the t-distribution. In this case, the degrees of freedom, called effective degrees of freedom, ν_{eff}, are calculated from a combination of each degree of freedom assumed for each uncertainty source. In this analysis, the equation below given by ISO GUM (ISO, 2008) is employed,

$$\nu_{eff} = \frac{u_c^4(y)}{\sum_{i=1}^{N} \frac{u_i^4(y)}{\nu_i}} \tag{17}$$

where u_c is the combined uncertainty, u_i are the standard uncertainty for each source i. The estimated degrees of freedom, ν_i, for each source i are

$$\nu_i = \left(\frac{1}{\frac{2\Delta u(x_i)}{u(x_i)}}\right)^{-2} \tag{18}$$

and $\Delta(x_i)/u(x_i)$ are expected relative uncertainties for each source i based on experience and scientific judgement (ISO, 2008).

By assuming values of 5% for relative uncertainties of air gap, wave amplitude and mooring line tension, the uncertainty of two measurements may vary about 10%. Therefore, the effective number of degrees of freedom for x'_3, x'_{ag} and T'_2 are 56.61, 77.85 and 68.62 , respectively.

The 95% confidence level coverage factor can then be determined by

$$k_{95} = t_{95}(\nu_{eff}) \tag{19}$$

This equation gives the coverage factors of 2.003, 1.991 and 1.995 for x'_3, x'_{ag} and T'_2, respectively.

In summary, the expanded uncertainties for a 95% confidence level were obtained in the Table 4.

Fig. 3 shows the full scale uncertainty bars in the measured RAO's of heave , air gap and mooring line tension at wave period of 10 seconds.

5.6. Discussions

For the heave, air gap and tension RAOs, the Type B analysis led to higher uncertainty values in comparison to uncertainties quantified in accordance with the Type A analysis. This is mainly caused by the difference in the analysis methodologies for Type A and Type B uncertainties. The Type A uncertainties are evaluated

by applying statistical methods to repeated measurements while the Type B uncertainties are estimated by scientific judgement based on the available information including the internal calibration procedure, precision of instruments provided by the manufacturers and the basin experience. Furthermore, the Type A analysis only considers the scattering of data obtained in repeated tests. If the test matrix were varied, for instance, including the use of different wave probes and motion tracking systems in the test matrix, the scattering of data would be greater. In this case, the uncertainty values calculated by the Type A analysis would increase and they would be similar to those obtained by using the Type B analysis.

According to the ISO recommendations (ISO, 2008), other identified uncertainty sources that are not included in the reduction equation should also be accounted for Type B uncertainties. For the sake of simplification, this has not been carried out in the present study. Further studies are needed. For instance, the uncertainties in the heave value due to the change of fluid density or an error in the model geometry should be taken into account in their standard uncertainties estimates, degrees of freedom and the partial derivatives in the reduction equation.

Following the ISO recommendations, the final uncertainty shall combine Type A and Type B results, i.e., the final u_c and u_e values should be calculated by using the equations as in ISO GUM - JCGM100 (ANNEX G, NOTE 3)(ISO, 2008).

6. Challenges ahead

It is a challenge to quantify the uncertainty sources in model tests, especially involving dynamic positioning systems and mooring/riser systems. A demonstration of this is the calculation of Type B uncertainties, which not only depends on the experience but also on the analysis methodology.

For model tests and numerical simulations involving highly nonlinear phenomena such as green water on deck, slamming, sloshing and wave run-up, it would be more difficult to quantify the uncertainties. Examples of recent experimental and numerical simulations of these phenomena include the work by Kaminski and Bogaert (2009), Kimmoun et al. (2009) and Bunnik and Huijsmans (2007).

Green water and air gap, representing the highly nonlinear effects, becomes important for the design/operation of offshore structures in extreme sea conditions. Accurate measurements of relative wave and impact load are important for the determination of design values and the development of reliable numerical method. The increase in the size of LNG ships in recent years, together with the development of floating storage and regasification units (FSRUs) operating in arbitrary filling conditions, have boosted a number of projects aiming at improving the design methodologies and the scientific knowledge about the physics of hydroelastic impact problems involving a complex containment system and the two phase flow of a liquefied gas as well as its gaseous phase. The tests and simulations of sloshing flow and load on structures are of importance.

These phenomena all involve multi-phase flows with water breaking and air bubbles. Their simulations and model tests potentially involve a higher level of uncertainties. A state-of-the-art-review of work on numerical simulations and model tests of these highly nonlinear effects can be found in the report of the ITTC Ocean Engineering Committee Report (ITTC, 2011). Using sloshing as one example, although progress has been made in the global simulation of the ship and liquid cargo coupled behavior, numerical simulation of local fluid–structure interaction effects during two-phase impacts and large-scale impact tests, the uncertainties in the simulation and tests are difficult to quantify. The difficulty in scaling also contributes to the level of uncertainty.

On the other hand, to quantify the uncertainties in extrapolation of model test results to full-scale, especially for problems where the potential-flow forces and viscous forces are both important, remains challenging in ocean engineering.

7. Conclusions

There are many parameters that may cause uncertainties in ocean engineering tests. In this paper, the parameters that may cause uncertainties in ocean engineering model tests, full-scale tests and numerical simulations are presented in terms of physical properties of the fluid, initial conditions, model definition, environment, scaling, instrumentation and human factors. Emphasis is given to the uncertainty sources in model tests involving deep-water mooring lines, risers and dynamic positioning systems and the need for quantifying them.

A methodology for uncertainty analysis is described according to ISO-GUM. As an example of application, the combined and expanded uncertainties in the model tests of a moored semi-submersible platform were assessed and quantified in terms of motion responses, air gap and mooring line tensions. The challenge of calculating Type B uncertainties has been demonstrated as the calculation not only depends on the experience but also on the analysis methodology. From the results obtained for Type A and Type B uncertainty analysis, it is concluded that the Type B uncertainty may play a more important role in model test results.

It is further concluded that the quantification of uncertainties may be challenging in model tests and numerical simulations of ocean and offshore structures, particularly in extrapolating model test results to full scale and utilizing complex numerical models.

More studies on applying the uncertainty analysis methodology in ocean engineering tests and numerical simulations are recommended.

References

Bunnik, T., Huijsmans, R., 2007. Large scale LNG sloshing model tests. In: Proceedings of the ISOPE2007, Lisbon, Portugal.

Elms, D.G., Brown, C.B., 2013. Intuitive decisions and heuristics – an alternative rationality. Civil Eng. Environ. Syst. 30 (3–4), 274–284.

Hirdaris, S.E., Bai, W., Dessi, D., Ergin, A., Gu, X., Hermundstad, O.A., Huijsmans, R., Iijima, K., Nielsen, U.D., Parunov, J., Fonseca, N., Papanikolaou, A., Argyriadis, K., Incecik, A., 2014. Loads for use in the design of ships and offshore structures. Ocean Eng. 78, 131–174.

Hussain, A., Nah, E., Fu, R., Gupta, A., 2009. Motion comparison between a conventional deep draft semi-submersible and a dry tree semi-submersible. In: Proceedings of the OMAE2009.

ISO, 2008, Guidance for uncertainties in measurement (GUM), JCGM100.

ITTC, 2011, Final Report and Recommendation to the 26th ITTC, Ocean Engineering Committee Report.

Kaminski, M., Bogaert, H., 2009, Full scale sloshing impact tests. Proceedings of the ISOPE2009, Osaka, Japan.

Kendon, T.E., Oritsland, O., Baarholm, R.J., Karlsen, S.I., Stansberg, C.T., Rossi, R.R., Barreira, R.A., Matos, V.L.F., Sales, J.S., Jr., 2008. Ultra-deepwater model testing of a semi-submersible and hybrid verification. In: Proceedings of the OMAE, Estoril, Portugal.

Kimmoun, O., Malenica, S., Scolan, Y.M., 2009. Fluid structure interactions occurring at a flexible wall impacted by a breaking wave. In: Proceedings of the ISOPE2009, Osaka, Japan.

Morgan, G.C.J., Zang, J., 2010. Using the rasInterFoam CFD model for non-linear wave interaction with a cylinder. In: Proceedings of the ISOPE 2010.

Ormberg,H., Stansberg, C.T., Yttervik, R., Kleiven, G., 1999. Integrated vessel and mooring analysis applied in hybrid model testing. In: Proceedings of the ISOPE1999, Brest, France.

Roos, J.S., Swan, C., Haver, S., Gudmestad, O., 2009. An experimental investigation of wave impacts on the deck of a gravity based structure. In: Proceedings of the OMAE2009, Honolulu, USA.

Roos, J., Swan, C., Haver, S., 2010. Wave impact on the column of a gravity-based structure. In: Proceedings of the OMAE2010, Shanghai.
Stansberg, C.T., Ormberg, H., Oritsland, O., 2002. Challenges in deep water experiments: hybrid approach. J. Offshore Mech. Arct. Eng. 124 (2), 90–96.
Tversky, A., Kahneman, D., 1974. Judgement under uncertainty-heuristics and biases. Science 185 (4157), 1124–1131.
Vassalos, D., 1999. Physical modelling and similitude of marine structures. Ocean Eng. 26 (2), 111–123.
Welch, P.D., 1967. Use of fast Fourier transform for estimation of power spectrum — a method based on time averaging over short modified periodograms. IEEE Trans. Audio Electroacoust. AU15, 70–73.
Yang, R.Y., Chen, H.H., Hwung, H.H., Jiang, W.P., Wu, N.T., 2010. Scour around the jacket type offshore wind turbine foundation in shallow water. In: Proceedings of the ISOPE2010, Beijing, China.